JOURNAL OF BACTERIOLOGY, July 1994, p. 3944–3955
0021-9193/94/$04.00+0

Vol. 176, No. 13

Promoter and Operator Determinants for Fur-Mediated Iron Regulation in the Bidirectional *fepA-fes* Control Region of the *Escherichia coli* Enterobactin Gene System

MARJORIE D. HUNT, GREGG S. PETTIS,† AND MARK A. McINTOSH*

Department of Molecular Microbiology and Immunology, University of Missouri, School of Medicine, Columbia, Missouri 65212

Received 5 November 1993/Accepted 30 April 1994

The *fepA-entD* and *fes-entF* operons in the enterobactin synthesis and transport system are divergently transcribed from overlapping promoters, and both are inhibited by the Fur repressor protein under iron-replete conditions. A plasmid harboring divergent *fepA'-'phoA* and *fes-entF'-'lacZ* fusions, both under the control of this bidirectional regulatory region, was constructed for the purpose of monitoring changes in expression of the two operons simultaneously. Deletion analysis, site-directed mutagenesis, and primer extension were employed to define both a single promoter governing the expression of *fes-entF* and two tandemly arranged promoters giving rise to the opposing *fepA-entD* transcript. A single Fur-binding site that coordinately regulates the expression of all transcripts emanating from this control region was identified by in vitro protection from DNase I nicking. The substitution of one base pair in the Fur recognition sequence relieved Fur repression but did not change the in vitro affinity of Fur for its binding site. Additional mutations in a limited region outside of the promoter determinants for either transcript inhibited expression of both *fes* and *fepA*. These observations suggest a mechanism of Fur-mediated regulation in this compact control region that may involve other regulatory components.

Bacteria adapt to environmental change by dramatic shifts in gene expression and protein production. In response to iron deprivation, most oxygen-metabolizing microorganisms produce and excrete small iron-chelating molecules called siderophores (36) and perform the specific transport functions required for the retrieval of their ferrated derivatives (41). *Escherichia coli* typically synthesizes and secretes the catechol-based siderophore enterobactin, and some isolates produce the hydroxamate derivative aerobactin, as well.

The genes required for enterobactin biosynthesis (*ent*) and transport (*fep*) map in a cluster at minute 13 (2) along with *fes* (for ferric enterobactin esterase); *fepE*, which encodes a protein of unknown function that is localized on the periplasmic side of the cytoplasmic membrane (13); and two other genes encoding uncharacterized protein products designated P15 (40) and P43 (50) to indicate their approximate sizes. Expression of the enterobactin system emanates from three regulatory regions containing divergently oriented promoters: one located between *fepB* and the *entCEBA(P15)* operon (8, 44), one between *fepD* and *P43* (50), and a third between *fepA* and *fes* (45). Except for *fepE*, which is constitutively expressed from its own weak promoter (13), the six transcripts arising from these three promoter regions encode all of the genes in the enterobactin gene cluster and are induced when the external iron supply becomes depleted (8, 22, 45, 50). This sensitivity to iron limitation is shared by the aerobactin system and other genes and operons throughout the chromosome (6, 30), many of which direct the transport of exogenously-derived siderophore species.

The global effector for the iron-mediated response is encoded by the *fur* locus at min 15.7 (3, 4, 30). When associated with ferrous iron in vivo, the 17-kDa Fur protein (31) represses expression of the iron acquisition systems by inhibiting transcription. Initial binding assays in vitro identified a 31-bp primary Fur-binding sequence in the aerobactin promoter, along with an adjoining 19-bp region that is only secondarily occupied at higher Fur concentrations (18). Subsequent hydroxyl radical footprinting of the aerobactin operator region led to the suggestion that Fur may wrap around the operator DNA, making multiple contacts at evenly spaced (usually A-T) doublets on all sides of the helix, with each protected doublet separated by four intervening base pairs (19). From comparative studies of the promoter regions of aerobactin and other iron-regulated genes (9, 18), a 19-bp dyad (5'-GATAAT GATAATCATTATC-3') within the primary protected region was proposed as a consensus Fur-binding sequence or "iron box." Two salient features of this sequence are its dyad symmetry and the regular phasing of A-T doublets throughout.

The apparent requirement for regular multiple contacts on all sides of the helix could explain why no single base-pair substitutions that relieve iron regulation have been isolated (8, 21), yet single-base deletions within the consensus operator can abolish its ability to dictate iron control (10).

Although the repressor protein was first recognized (and named) as a ferric iron uptake regulator, it is now known to serve a more general role as a sensor of iron availability in the cell and a repressor of other genes that are not directly involved in the procurement of iron. The Fur regulon in *E. coli* includes, besides genes required for iron acquisition, genes for virulence determinants such as the colicin I receptor (28) and Shiga-like toxin (9), Mn-superoxide dismutase (42), and *fur* itself (20). Fur is the only known regulator of the iron import genes, but in some other genes in the regulon (17, 20, 32) and

* Corresponding author. Mailing address: Department of Molecular Microbiology and Immunology, M653 Health Sciences Center, University of Missouri, Columbia, MO 65212. Phone: (314) 882-4133. Fax: (314) 882-4287. Electronic mail address: mam@medsci.mbp.missouri.edu.

† Present address: Department of Genetics, Stanford University School of Medicine, Stanford, California 94305.

TABLE 1. Primers used in this study

Primer	Sequence	Location (5′→3′)[a]
P7	5′-GGG AAT GAA GCT TCT TGT T-3′	−214→−196
P9	5′-CGC TTT ATC CTC GAG TAT T-3′	+195→+177
M1	5′-TTT CAT TAA TTG CAG AAA TAT-3′	+22→ +2
M4	5′-TTT TCA TTG ATT ACA GAA ATA T-3′	+23→ +2
M6	5′-TTT TCA TTA ATT ACA GAA ATA T-3′	+23→ +2
M7	5′-GAT CCT GAA AGA CAC GCA GTG CA-3′	−82→−104
M8	5′-TGG GTG AGC AAA AAC AGG AAG G-3′	
M9	5′-AAT ATT AAT GAT AAC TAT TTG C-3′	−6→ −27
M10	5′-AAT AGC GGA ATG GCG CG-3′	−34→ −50
P13	5′-TTG ATA ACT ATT GCA CGT TGC AAT AGC GT-3′	−13→ −41
P14	5′-ATT GAT TGC AGA CCA CGA TTG ATA ATA TT-3′	+18→ −11
P16	5′-TTG CAT TTG TAA TAG CGT A-3′	−24→ −42

[a] Relative to the *fes* transcription start site.

in at least two other species (27, 47), it appears to work in conjunction with other regulators to modulate gene expression. Control of the *sodA* gene in *E. coli*, for instance, involves not only Fur but five other global regulators: two positive effectors and three other repressors, including another iron-dependent regulatory protein, Fnr (17).

The region between the *E. coli fepA* and *fes* genes contains overlapping, divergently oriented promoters. One message originating from this junction encodes the *fes* and *entF* genes separated by the short, uncharacterized open reading frame ORF1 (45). The opposing transcript contains the *fepA* and *entD* genes (1, 45). Earlier primer extension studies (45) led to the identification of probable transcription start sites in each direction and, from that, the assignment of putative −35 and −10 promoter determinants controlling the expression of these genes. Initial characterization of the intercistronic region also allowed the identification of four overlapping nucleotide stretches, designated *fepA* I and II and *fes* I and II, with sequence similarity to the consensus iron box (45).

This report describes the further characterization of the iron-regulated promoters governing the expression of the *fepA* and *fes* operons. We have constructed a bidirectional fusion plasmid and used it to monitor the functional effects of deletions and base substitutions within the regulatory region. Direct analysis of the transcripts arising from these promoters has been used to corroborate the functional studies, allowing the identification of an additional *fepA* promoter element that appears to be the primary functional promoter for this gene under the conditions that we were examining. Using DNase I protection and gel-retardation assays with purified Fur protein, we have characterized the interaction of the repressor protein with its binding site and identified a single operator element that governs the expression of the *fes* and both *fepA* transcripts simultaneously.

Because the operons overlap so extensively in the *fepA-fes* control region, they differ from the Fur-regulated transcripts characterized to date. Our results suggest a degree of complexity in the transcriptional regulation of these two operons that may implicate other regulatory factors.

MATERIALS AND METHODS

Bacterial strains, plasmids, bacteriophage, and primers. *E. coli* CC118 (*lacZ phoA recA*) (38) was used as the host for all fusion plasmids. Strain JM101 (43) served as the host for M13 bacteriophage recombinant derivatives. For site-directed mutagenesis, strain CJ236 (*ung dut*), obtained from Bio-Rad Laboratories (Richmond, Calif.), was used for the isolation of uracil-containing M13 templates. Strain XL1-Blue (Stratagene, La Jolla, Calif.) served as a host for plasmids derived from Bluescript vectors.

All bidirectional fusion plasmids were derivatives of the pBR322-based *lacZ* fusion vector pMC1403 (11). For in vitro transcription of RNA probes used in RNase protection experiments, the 385-bp *Xho*I-*Hin*dIII fragment of pITS343-0 (see below) was moved into the Bluescript vector KS$^-$ (Stratagene).

The M13 bacteriophage derivatives M13mp18 and M13mp19 (43) were used in the construction and nucleotide sequencing of site-specific mutations. The vector λ Tn*phoA*, a gift from Colin Manoil, delivered the Tn*phoA* transposable element for the construction of *phoA* gene fusions (38).

Oligonucleotide primers were synthesized by the University of Missouri DNA Core Facility on a model 380B DNA synthesizer (Applied Biosystems, Inc., Foster City, Calif.). The primers used in this study are listed in Table 1. Mismatched bases for mutagenesis are underlined, and primer locations indicated are relative to the *fes* transcription start site shown in Fig. 2. Primer M8 was used in the primer extension of the plasmid-encoded β-lactamase gene whose product served as an internal control in the quantitation of *fepA* primer extension products.

General genetic methods and nucleotide sequencing. Isolation of plasmid and single-stranded M13 DNA, as well as nucleotide sequencing of both single- and double-stranded templates, were described previously (44, 45). Cells were transformed or transfected by the method of Cohen et al. (15) or the simplified transformation procedure of Hanahan (29).

Sequencing, primer extension, RNase protection, and footprinting reactions were analyzed on 6 or 8% polyacrylamide-urea sequencing gels, which were exposed without drying to Kodak XRP-5 film at −70°C.

Enzyme assays. CC118 harboring one of the reporter plasmids was grown to early log phase in Luria-Bertani broth supplemented with 100 μg of ampicillin per ml and either 20 μM $FeSO_4$ plus 10 mM sodium citrate to guarantee an iron surplus or 200 μM 2,2′-dipyridyl to create conditions of iron starvation. The cells were permeabilized by using $CHCl_3$ and 0.1% sodium dodecyl sulfate and were assayed for β-galactosidase activity (39) or alkaline phosphatase expression (7). In both cases, samples were centrifuged for 5 min at 12,000 to 14,000 × *g* before the optical density (OD) was measured. This allowed the omission of the OD_{550} adjustment for light scattering and provided more consistent results.

We have observed that the absolute values obtained can vary somewhat from day to day on the basis of differences in batches

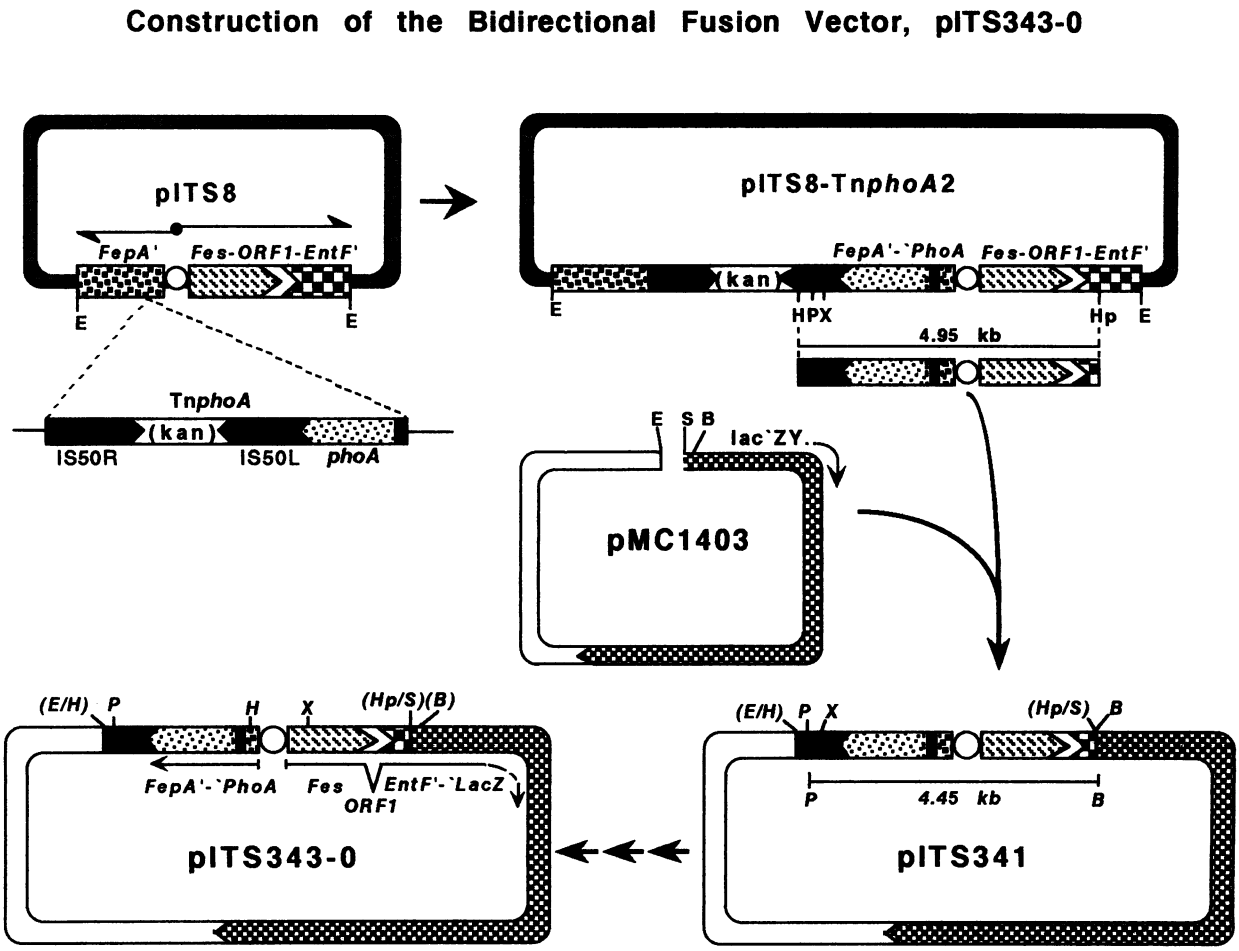

FIG. 1. The bidirectional fusion vector pITS343-0. Details of construction have been given in the text. The fill pattern for each individual component involved in the construct (not drawn to scale) is consistent throughout the figure. Only relevant enzyme sites are shown: E, *Eco*RI; H, *Hin*dIII; P, *Pst*I; X, *Xho*I; Hp, *Hpa*I; S, *Sma*I; and B, *Bam*HI. The three-step transition from pITS341 to pITS343-0 entailed the removal of an unwanted *Xho*I site in IS*50*L, the creation of new *Xho*I and *Hin*dIII sites flanking the promoters, and the end-filling of the pMC1403 *Bam*HI site to put the *fes'-'lacZ* fusion in frame. The 4.45-kb *Pst*I-*Bam*HI fragment of pITS341 was used for in vitro mutagenesis of the regulatory region as described in the text.

of media, incubator conditions, or exact growth stages at which the cells are harvested, etc. Within a set of experiments performed on the same day, however, expression from the various promoter and operator mutants, relative to the wild type, remains constant. The enzyme assay results presented in Fig. 2B and 3B are the averages obtained from experiments performed on days when all of the fusion constructs could be assayed at the same time in the same medium under exactly the same conditions.

Isolation of an iron-regulated fepA'-'phoA fusion and construction of the bidirectional fusion vector pITS343-0. Isolation of an in-phase fusion between *fepA* and the structural gene (*phoA*) for alkaline phosphatase was accomplished by using the vector λ Tn*phoA* and the target plasmid pITS8, in strain CC118. The 3-kb pITS8 insert (Fig. 1) includes the 5′ end of the *fepA* gene, its iron-regulated promoter region, and the 5′ portion of the divergently oriented *fes-entF* transcript (23). Clones with Tn*phoA* insertions were generated by the method of Manoil and Beckwith (38) and were selected on iron-poor Luria-Bertani agar containing 50 μg of ampicillin per ml, 50 μg of kanamycin per ml, and 40 μg of 5-bromo-4-chloro-3-indolyl-phosphate *p*-toluidine salt (XP) per ml. Insertion sites were determined by restriction endonuclease mapping followed by nucleotide sequencing. One clone, pITS8-Tn*phoA*2 (Fig. 1), displayed iron-regulated alkaline phosphatase activity and produced a hybrid FepA'-'PhoA protein of M_r 55,000 in *E. coli* minicells (data not shown).

For construction of a bidirectional fusion vector, pITS8-Tn*phoA*2 was digested with *Hin*dIII and *Hpa*I, producing a 4.95-kb fragment (Fig. 1) that extended from a *Hin*dIII site in IS*50*L, downstream of the *fepA'-'phoA* fusion, to the *Hpa*I site in *entF* used for previous *entF'-'lacZ* fusion constructions (46). This fragment was end-filled by using the Klenow fragment of DNA polymerase I and was ligated into *Eco*RI-*Sma*I-digested (and end-filled) pMC1403 vector. The resulting clone, pITS341 (Fig. 1), was identified as an alkaline phosphatase-producing clone with its insert in the appropriate orientation (*entF* sequences fused to the *lacZ* gene). In order to create the in-phase *entF'-'lacZ* fusion pITS342, the vector *Bam*HI site at the *entF-lacZ* junction was digested, filled, and ligated as described previously (46). In a similar manner, a *Xho*I site within the Tn*phoA* sequence of pITS341 was removed (pITS341-δX) to allow for the subsequent creation of a unique *Xho*I site in the *fes* gene.

Site-directed mutagenesis. Site-directed mutations were generated by using the uracil-containing template method of Kunkel (35) and the Muta-Gene M13 in vitro mutagenesis kit and protocol supplied by Bio-Rad. For the creation of a *Hin*dIII-*Xho*I promoter cassette, the 4.45-kb fragment of pITS341-δX, spanning from a *Pst*I site in IS*50*L of Tn*phoA* to the *Bam*HI site at the *entF-lacZ* junction, was subcloned into the vectors M13mp18 and M13mp19. After passage of the recombinant phage in strain CJ236, primers P7 and P9 were used sequentially to create new *Hin*dIII (P7) and *Xho*I (P9) sites on either side of the promoter region. The presence of newly created restriction sites was verified by relevant restriction endonuclease mapping of replicative form DNA. The *Pst*I-*Bam*HI fragment containing both new restriction sites was ligated back into the *Pst*I-*Bam*HI-cut pITS341 vector, creating a clone with unique *Hin*dIII and *Xho*I sites, separated by 385 bp and flanking the *fepA-fes* intercistronic region. Digestion with *Bam*HI, end-filling, and ligation (as for pITS342) created the double fusion derivative pITS343-0.

Site-specific operator and promoter mutations were created in the same manner, except that oligonucleotides containing 1- to 5-bp central mismatches were annealed to a uracil-containing template that contained the newly created *Hin*dIII and *Xho*I sites. Clones with the desired mutations were identified by nucleotide sequencing of their single-stranded templates. Replicative form DNA from the desired clones was digested with *Hin*dIII and *Xho*I, the 0.4-kb fragment containing the *fepA-fes* intercistronic region was cloned back into similarly digested pITS343-0, and the sequence of the *Hin*dIII-*Xho*I insert in each reconstructed plasmid was again verified to assure that no unwanted changes had been introduced.

Deletion constructions. Twenty-five μg of pITS343-0 was linearized at either its unique *Hin*dIII or *Xho*I restriction site, and nested *Bal*31 deletions were generated essentially as described by Sambrook et al. (49). At 30-s intervals, 2-μg aliquots were removed and the enzyme was inactivated. Samples were recircularized by ligation, digested to completion with the enzyme originally employed to linearize the plasmid, and reintroduced into strain CC118. For deletion mapping of the promoter controlling *fes-entF'-'lacZ*, transformants were screened on MacConkey lactose medium containing 50 μg of ampicillin per ml and 200 μM 2,2'-dipyridyl. For analysis of the promoter controlling expression of the *fepA'-'phoA* fusion, transformed cells were plated on nutrient agar (8 g of nutrient broth [Difco] and 5 g of NaCl per liter) containing ampicillin, XP, and 200 μM 2,2'-dipyridyl. The boundary of each selected deletion was determined by restriction endonuclease mapping and nucleotide sequencing of individual clones.

Primer extension and nuclease protection of the *fepA* transcript. Protocols for RNA isolation and kinasing of primers have been described previously (45). End-labelled primer (250 fmol of primer M7) was annealed to 10 to 30 μg of total cellular RNA isolated from CC118 cells, grown under low-iron conditions, that harbored pITS343-0 or one of its mutant derivatives. Primer extension analyses were done by the method of Fouser and Friesen (24) with the minor modifications described by Pettis et al. (45). If the primer extension products were to be quantitated, 250 fmol of primer M8, complementary to β-lactamase mRNA, was added to each reaction mixture as an internal control.

RNase protection experiments were done essentially as described by Clemens and Pintel (14). To generate RNA probe, the *Hin*dIII-*Xho*I fragment of pITS343-0 was subcloned into Bluescript KS$^-$ and digested with *Ssp*I, producing a linear fragment to be used as a template for T7 RNA polymerase (RNAP). Approximately 0.5 μg of the resulting probe and 10 μg of total cellular RNA were annealed, and the RNA hybrids were digested by using RNase A and T1 at concentrations of 10 μg/ml and 50 ng/ml, respectively.

Undried polyacrylamide-urea gels were wrapped and exposed to storage phosphor screens (Eastman Kodak, Rochester, N.Y.). The relative intensity of the individual bands was determined with Imagequant version 3.0 software and a model 400A PhosphorImager purchased from Molecular Dynamics (Sunnyvale, Calif.).

Footprint analysis and gel-retardation assays. The 0.4-kb *Hin*dIII-*Xho*I fragment from pITS343-0 or its mutant derivatives was isolated and labelled at the *Hin*dIII end by using modified T7 DNA polymerase (Sequenase, version 2; United States Biochemical Corp., Cleveland, Ohio) and α-^{32}P[dATP] (3,000 Ci/mmol) as the only nucleotide. Purified Fur protein was kindly supplied by J. B. Neilands. DNase I protection protocols were based on the procedure of de Lorenzo et al. (18) but using 100 μM Mn^{++} as the Fur-activating divalent metal ion since it exhibits properties similar to Fe^{++} but is more stable in the presence of oxygen. The details of the footprinting procedure have been described previously (8). A dideoxy sequence ladder generated with primer P9 was employed as a size marker to determine the precise location of the protected regions.

Gel-retardation assays (25, 26) were performed as described by de Lorenzo et al. (19), again by using purified Fur protein in conjunction with 100 μM Mn^{++}. Each binding reaction contained 0.1 pmol of the labelled *Hin*dIII-*Xho*I fragment from pITS343-0, pITS343-13, or pITS343-16 and varying concentrations of Fur in a volume of 20 μl. Fur-bound fragments were separated from unbound DNA on 8% nondenaturing polyacrylamide gels (75:1 acrylamide:*N*,*N*-methylenebisacrylamide) run at 200 V for 3 to 4 h. Dried gels were exposed to Kodak XRP-5 film at −70°C and, subsequently, to storage phosphor screens for quantitation of bands as described above.

RESULTS

Construction of a bidirectional fusion vector. The overlapping nature of the promoters located in the *fepA-fes* intercistronic region raised the possibility that certain portions of this sequence may regulate both transcripts simultaneously. In order to monitor all regulatory effects elicited by alterations in this region, a bidirectional fusion vector was constructed. Because previous work in our laboratory indicated that Fur activity is not titrated out in the presence of operators carried on multicopy plasmids (8, 34), a pBR322-based construct was employed. The transposable element Tn*phoA* (38) was inserted into the *fepA* gene carried on pITS8 (Fig. 1), yielding a chimeric *fepA'-'phoA* gene. Nucleotide sequencing of this construct, pITS8-Tn*phoA*2, revealed that the transposon was inserted 1 bp after the 24th codon of *fepA* (37), producing a 450-amino acid fusion protein with iron-regulated alkaline phosphatase activity.

The *Hin*dIII-*Hpa*I fragment containing this *fepA'-'phoA* fusion, *fes*, and part of *entF* was subcloned into pMC1403 (11) to give pITS341 (Fig. 1). End filling of the *Bam*HI site of pITS341, like previous *entF'-'lacZ* fusion clones, permits the production of a hybrid EntF'-'LacZ protein of M_r 120,000 (46). The new clone (pITS342; data not shown) displays iron-regulated alkaline phosphatase activity as a result of the *fepA'-'phoA* fusion and iron-regulated β-galactosidase activity due to expression of the *entF'-'lacZ* fusion. Both of these are under the control of the bidirectional regulatory region situated between *fepA* and *fes* (45, 46).

Unique *Xho*I and *Hin*dIII restriction sites flanking this

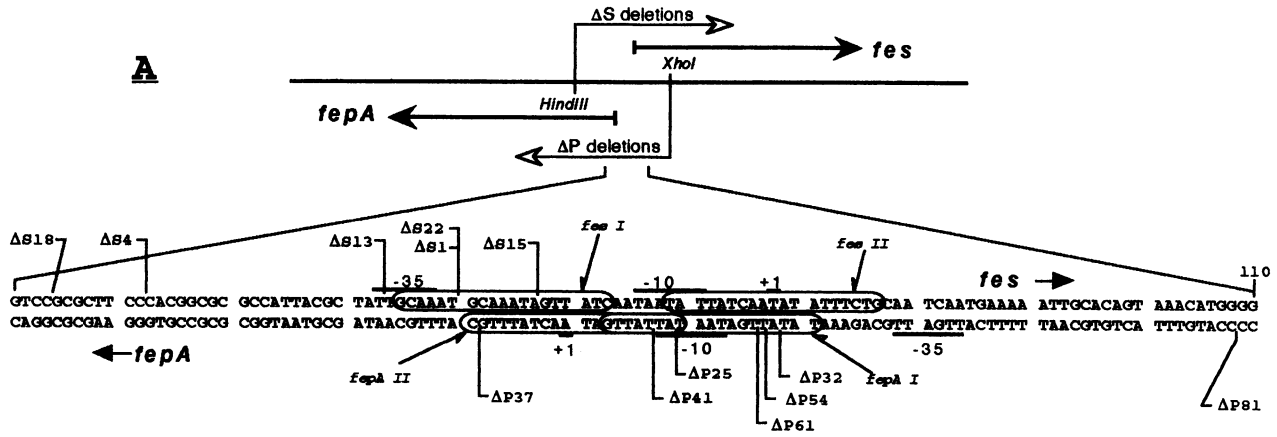

B

ΔS Clone	Endpoint	β-galactosidase Activity (U) +Fe	β-galactosidase Activity (U) -Fe	Induction (-Fe/+Fe)	ΔP Clone	Endpoint	Alkaline Phosphatase Activity (U) +Fe	Alkaline Phosphatase Activity (U) -Fe	Induction (-Fe/+Fe)
pITS343-0	---	68	980	14.4	pITS343-0	---	132	783	5.9
S18	-63	77	942	12.2	P81	-58	138	771	5.6
S4	-54	64	928	14.5	P32	-18	21	272	12.9
S13	-34	3	12	4.0	P54	-17	37	217	5.9
S1	-27	47	81	1.7	P61	-15	88	319	4.2
S22	-27	8	9	1.1	P25	-10	79	286	3.6
S15	-19	13	16	1.2	P41	-8	38	103	2.7
					P37	+9	13	18	1.4

FIG. 2. Deletion analysis of the *fepA* and *fes* promoters. (A) Schematic representation of the *fepA-fes* promoter region and the enzyme sites which served as deletion origins. The sequence of the central portion of this region is shown below along with the precise endpoints of deletions originating at the *Xho*I site (ΔP) or the *Hin*dIII site (ΔS). The previously proposed *fepA* promoter (45) is underlined, and the *fes* promoter determinants are overlined. The circled sequences constitute the four potential operator sites (45): on the top strand *fes* I (left) and *fes* II (right) are marked, and *fepA* II (left) and *fepA* I (right) are indicated on the lower strand. (B) β-galactosidase expression from the *fes-entF'-'lacZ* fusion and alkaline phosphatase activity from *fepA'-'phoA*, both expressed in Miller U, and iron-mediated induction ratios produced by the wild-type regulatory region (pITS343-0) or its deletion derivatives. Deletion endpoints specified in the table refer to the transcription start sites of *fes* (for ΔS deletions) and *fepA* (for ΔP deletions) proposed by Pettis et al. (45). Average standard deviations for the data presented here and in Fig. 3 are 9.2% of the given value for values >100 and 11% for values <100.

region were introduced by site-directed mutagenesis to create a movable cassette for manipulation of the *fepA-fes* intercistronic sequence. The introduction of the new enzyme sites results in an isoleucine-to-leucine amino acid change at position 5 of the FepA signal sequence (37) and a threonine-to-arginine change at the 19th amino acid of Fes (45). Neither mutation had a significant effect on the iron-regulated expression of alkaline phosphatase or β-galactosidase in the resulting clone, pITS343-0 (data not shown). This clone also retained a Fes^+ phenotype as judged by the complementation assay described previously (46).

Deletion analysis of the *fepA-fes* promoter region. To define the promoter and operator sequences essential for normal iron-regulated expression, a 5′ deletion map of each promoter was constructed. In the case of the *fes-entF* promoter, pITS343-0 was linearized at its *Hin*dIII site within *fepA*, treated progressively with *Bal*31 exonuclease, and religated. Clones exhibiting varying patterns of β-galactosidase expression on low-iron MacConkey lactose medium were chosen for analysis. The resulting deletions (ΔS series, Fig. 2A) were assayed for their magnitude of β-galactosidase expression under high- and low-iron conditions (Fig. 2B). Deletion up to position −54 (ΔS4) relative to the major transcription start site upstream of *fes* (45) does not significantly alter expression. However, deletion to position −34 (ΔS13) decreased maximal expression roughly 80-fold, while the induction ratio dropped from 14 to 4. Since the original T residue at base position −35 is now replaced by a G residue in the ΔS13 deletion junction (data not shown), this result is consistent with the previous postulate (45) that the 6-bp nucleotide stretch beginning at −35 (TTGCAA) is the essential −35 promoter determinant in this direction. Deletions farther into the *fes-entF* promoter region, to positions −28 (ΔS5; data not shown), −27 (ΔS1 and ΔS22), −22 (ΔS11; data not shown), and −20 (ΔS15) also greatly diminish expression and reduce the induction ratio to a very low level. The somewhat enhanced activity of deletion clone ΔS1, whose maximum expression increases approximately sevenfold relative to ΔS13, is most likely due to the creation of a new −35-like nucleotide stretch at its deletion junction, which retains the most conserved base positions of this promoter element (33) but at a suboptimal spacing relative to the rest of the promoter (data not shown). Taken together, these results confirm the relative position of the *fes-entF* promoter, do not implicate additional intercistronic sequences upstream of this

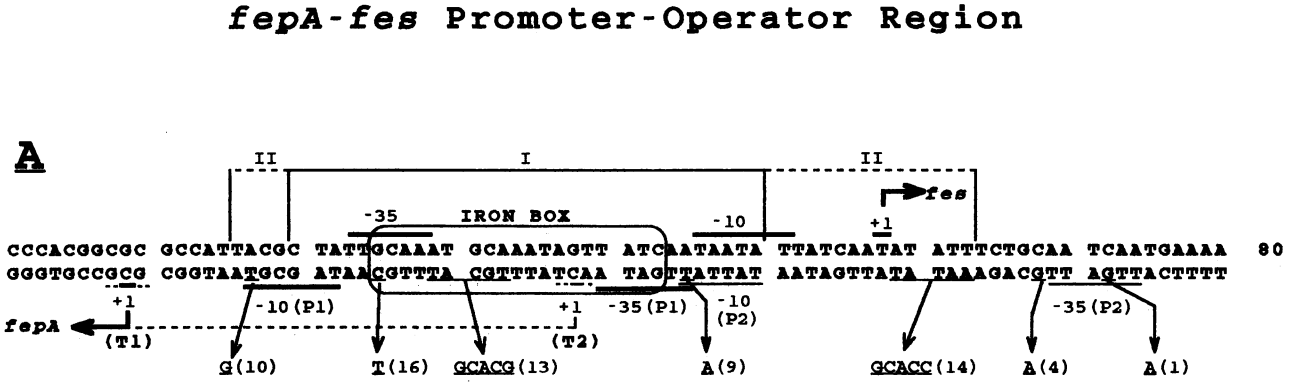

B

Clone	β-galactosidase +Fe	β-galactosidase -Fe	Induction (-Fe/+Fe)	Phosphatase +Fe	Phosphatase -Fe	Induction (-Fe/+Fe)
pITS343-0	68	980	14.4	132	783	5.9
pITS343-1	54	943	17.4	125	713	5.7
pITS343-4	88	980	11.1	133	759	5.7
pITS343-4.1	74	957	12.9	113	723	6.4
pITS343-9	29	933	32.2	4	39	9.8
pITS343-10	81	1090	13.5	18	180	10.0
pITS343-13	733	1054	1.4	657	755	1.1
pITS343-14	39	590	15.1	70	644	9.2
pITS343-16	5	7	1.4	565	793	1.4

FIG. 3. Mutational analysis of the bidirectional promoter region between *fes* and *fepA*. (A) Sequence of the central portion of the *fepA-fes* intergenic region showing the major regulatory determinants. At the top, the primary (I) and secondary (II) Fur-protected regions are marked. The sequence proposed as the functional iron box is enclosed. Site-specific mutations introduced into this sequence are shown below with the numerical suffix that defines each mutant clone in parentheses. The promoter determinants and transcription start sites for *fes* are overlined and those for *fepA* (P1 and P2), as we have redefined them, are underlined. Some ambiguity in the precise transcription start sites determined by primer extension analysis (see Fig. 4 and 5) are indicated by dotted lines. (B) The expression of β-galactosidase activity from the *fes* promoter and alkaline phosphatase from the *fepA* promoters, and the iron-mediated induction ratios generated from pITS343-0 and its mutant derivatives.

region as being major contributors to expression in this direction, and show that sequences between the −35 and −10 elements of this promoter are essential for its iron control.

Deletion analysis for the *fepA-entD* promoter was similarly initiated by digesting pITS343-0 at the unique *Xho*I site in *fes* and treatment with *Bal*31 exonuclease. Each selected clone in this series (ΔP, Fig. 2A) was then quantitatively analyzed by measuring alkaline phosphatase activity under varying iron conditions (Fig. 2B). Most of the clones examined had been deleted to or through the presumed promoter region. Deletions to −18 (ΔP32), −17 (ΔP54), and −10 (ΔP25) are reduced in maximal expression relative to pITS343-0, but only by two- to threefold. Deletion as far as −8 (ΔP41) reduces the maximum expression by eightfold relative to the wild-type construct, but phosphatase activity is still significant. It is not until the deletions reach past the previously-designated *fepA* promoter and transcription start site (ΔP37) that phosphatase expression falls to near-background levels. Additionally, though these deletions impinge upon two of the potential Fur-binding sites (45; Fig. 2), most of the ΔP clones remain significantly iron regulated, suggesting that the sequences most critical for iron control in this direction are located further downstream. A reasonable location might be the adjacent region within the *fes-entF* promoter that resembles the consensus iron box sequence (18) and appears to be the key element in iron regulation of the *fes* transcript as well.

Quantitation of the effects of specific promoter and operator mutations. In an effort to corroborate and extend the results of the deletion studies, site-directed mutagenesis was employed to alter potentially important regulatory regions.

The deletion analyses described above and previous primer extension experiments (45) suggested that the sequence TTGCAA occupying positions 23 to 28 in Fig. 3A was the functional −35 determinant for *fes*. Because the G is a highly conserved component of the consensus σ^{70} −35 sequence (33), a C-to-T substitution in the antisense strand was made to change this sequence to TTACAA (pITS343-16). Like the S13 deletion, this change abolishes expression from the *fes-entF'-'lacZ* transcript (Fig. 3B), further supporting the assignment of this sequence as an important component of the promoter for *fes* and *entF*.

Similarly, on the basis of previous primer extension experiments performed on the *fepA* transcript (45), the sequence TTGATT on the *fepA* coding strand, occupying positions 74 to 69 in Fig. 3A, was changed to TTAATT (pITS343-1). This mutation, however, had little effect on the expression of the *fepA'-'phoA* transcript (Fig. 3B).

The assignment of this particular 6-base sequence as the functional −35 promoter element was based on primer extension studies and sequence analysis which showed it to be well spaced with respect to a perfect consensus −10 element (33) and a strong start site (45). However, we have noted previously, by comparing our sequence of this region with the consensus σ^{70} promoter, that multiple overlapping promoters

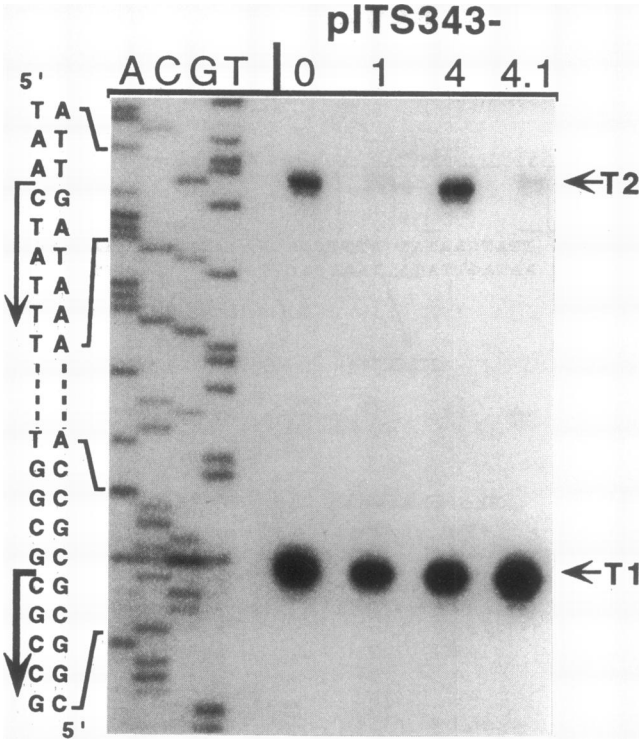

FIG. 4. Primer extension analysis of the *fepA'-'phoA* transcripts from pITS343-0, pITS343-1, pITS343-4, and pITS343-4.1. Primer M7 was used to generate the sequence ladder shown and the primer extension products in the four lanes on the right. RNA template was isolated from iron-starved CC118 cells harboring pITS343-0 or one of the three mutant derivatives indicated at the top. Bands labelled T1 and T2 represent transcripts arising at the promoters designated P1 and P2, respectively, in Fig. 3. The predominant start site for each transcript is illustrated on the partial sequence shown on the left.

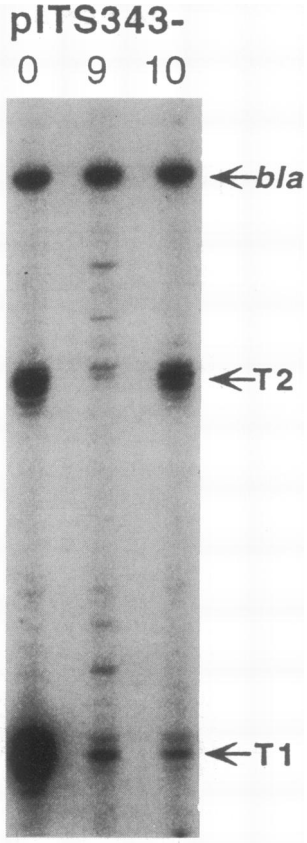

FIG. 5. Primer extension analysis of *fepA'-'phoA* transcripts from pITS343-0, pITS343-9, and pITS343-10. The primer extension products were generated as described in the legend to Fig. 4 from transcripts of pITS343-0 and the two mutant derivatives indicated at the top. Primer M8, which produces a 95-base extension product from β-lactamase (*bla*) RNA, was also included in each of these reaction mixtures, to allow standardized quantitation of the extension products.

might be functioning in the *fepA* direction (45). In light of the alkaline phosphatase data from pITS343-1 and the deletion mutants, the possibility of other functional promoters was investigated.

A second potential promoter determinant (TTGCAG, at positions 70 to 65 in Fig. 3A) overlaps by 2 bases the one initially identified and, like the first, is upstream of a heavily AT-rich region which could provide a suitable −10 element. To determine whether this sequence is serving as the −35 region for the *fepA* transcript, it was changed to TTACAG, both alone (pITS343-4) and in conjunction with the pITS343-1 mutation (pITS343-4.1). With both of these sequences altered away from consensus, however, strong phosphatase activity of the FepA'-'PhoA fusion protein persists (Fig. 3B). Primer extension on transcripts from pITS343-1, pITS343-4, and pITS343-4.1 (Fig. 4) indicates that the hexamer first chosen as the −35 element is, in fact, responsible for the production of an iron-regulated *fepA* transcript (T2 in Fig. 4) and that this transcript is eliminated by the pITS343-1 mutation. The mutation in the second hexamer has no effect. However, another very abundant iron-regulated band migrating lower in the gel (T1 in Fig. 4) is present in all four lanes. Quantitation of the relative intensity of the upper and lower fragments from cells harboring the wild-type regulatory region (pITS343-0) indicated that T1 accounts for a consistent 83.4(±0.9)% of the *fepA* message. Its intensity does not appear to be diminished by the pITS343-1 mutation. The apparent endpoint of this fragment falls within an area of GC-rich dyad symmetry (45; Fig. 4), and we had initially thought that it represented a premature reverse transcriptase termination site engendered by the folding of the RNA molecule. However, its persistence even in the absence of the longer transcript suggested that it might represent another transcription start site. RNase protection of the *fepA'-'phoA* transcript was employed to clarify the primer extension results, since this procedure is not as vulnerable to the problem of RNA secondary structure. In those experiments (data not shown), both the longer (T2) and shorter (T1) fragments were maintained with the same relative abundance that was produced by primer extension. This suggests that T1 in Fig. 4 is not a reverse transcriptase artifact.

Putative −35 (TTGATA, positions 45 to 40 in Fig. 3A) and −10 (TAGCGT at positions 22 to 17) elements for this promoter were identified and altered to ATGATA (pITS343-9) and TAGCGC (pITS343-10), respectively. Either of these mutations, standing alone, is sufficient to reduce phosphatase expression significantly (Fig. 3B), indicating that the shorter transcript is the major source of *fepA'-'phoA* expression. Primer extension of the pITS343-9 and pITS343-10 transcripts supported this conclusion (Fig. 5): both mutations curtail transcription from the downstream promoter, now designated P1. Interestingly, the single-base change of pITS343-9 has two other effects: it increases the induction ratio (low Fe:high Fe) in the *fes*

direction by more than twofold, from ~14 to ~32 (Fig. 3B), and it eliminates transcription from the upstream promoter, P2 (Fig. 5). The latter observation is reflected in markedly lower phosphatase activity from pITS343-9 in Fig. 3B when compared with that from pITS343-10. The simplest explanation for the simultaneous effect on P2 is that the functional P2-10 determinant is the sequence TATTAT that encompasses base positions 50 through 45 in Fig. 3A and not the previously designated TAATAT hexamer at positions 53 to 48. The pITS343-9 mutation, therefore, disrupts both promoters, virtually eliminating transcription of *fepA*.

Location of the iron-responsive operator sequence. Within the *fepA-fes* intercistronic region, we (45) had previously identified four potential iron-regulated operator sites on the basis of their similarity to the consensus Fur-binding sequence (18). The locations of these regions, designated *fepA* I and II on the *fepA* coding strand and *fes* I and II on the strand encoding *fes* (45), are illustrated in Fig. 2. The clustering of several possible binding sites in the promoter region and their overlapping nature suggested that alternate Fur-binding properties may regulate the relative iron-inducibility of these two transcripts. Earlier analysis of the aerobactin promoter led to the proposal that multiple contact points had to be disrupted in order to significantly affect Fur binding (19), and so a similar approach was chosen here. Two 5-bp changes were generated (Fig. 3A), each designed to alter multiple conserved base positions relative to the consensus iron box for two of the overlapping operator-like sequences (i.e., pITS343-13 has a mutation introduced into *fes* I and *fepA* II simultaneously, while pITS343-14 harbors a 5-bp mutation affecting both *fes* II and *fepA* I).

The pITS343-14 mutation has little effect on the ability of Fur to repress expression of either transcript in iron-replete medium, showing normal induction levels (low Fe:high Fe) of both phosphatase and β-galactosidase expression. pITS343-13, on the other hand, retains little iron repression capability, reducing the induction ratios to less than 2 in either direction (Fig. 3B). This suggests that a single Fur-binding site in the vicinity of the *fes* and *fepA* P1 −35 regions is responsible for Fur-mediated repression, consistent with the information provided by the deletion clones.

DNase I footprinting experiments using purified Fur repressor protein allowed a more detailed look at the operator binding site. At Fur concentrations as low as 10 nM (Fig. 6), the 0.4-kb *Hin*dIII-*Xho*I fragment from the wild-type clone contains a single 31-bp protected region spanning bases 20 to 50 in Fig. 3. At higher Fur concentrations—80 nM or above—the protected region expands in both directions to encompass an additional 17 bp (Fig. 6) in a manner similar to that described previously for the *iucA* (18) and *entC* (8) operators. The primary protected region encompasses a 19-base sequence that resembles the consensus iron box and is situated symmetrically between the two major promoters in the region. Although this sequence displays little of the dyad symmetry proposed to play a role in Fur binding, it does possess the conserved phasing of A-T doublets separated by four bases (----AT----AT----AT-) whose 3′ bonds are protected by Fur from hydroxyl radical nicking and must therefore represent contact points between Fur and the operator (19).

The pITS343-14 mutation lies within the area of secondary protection but outside the area shielded most strongly by Fur, and consistent with the enzyme assay data reported in Fig. 3, this mutant shows no alteration in the wild-type Fur-binding pattern (Fig. 7). In contrast, pITS343-13, with a 5-bp alteration in the central part of the primary protected region, shows an 8- to 16-fold reduction in affinity for the Fur protein (Fig. 7). No

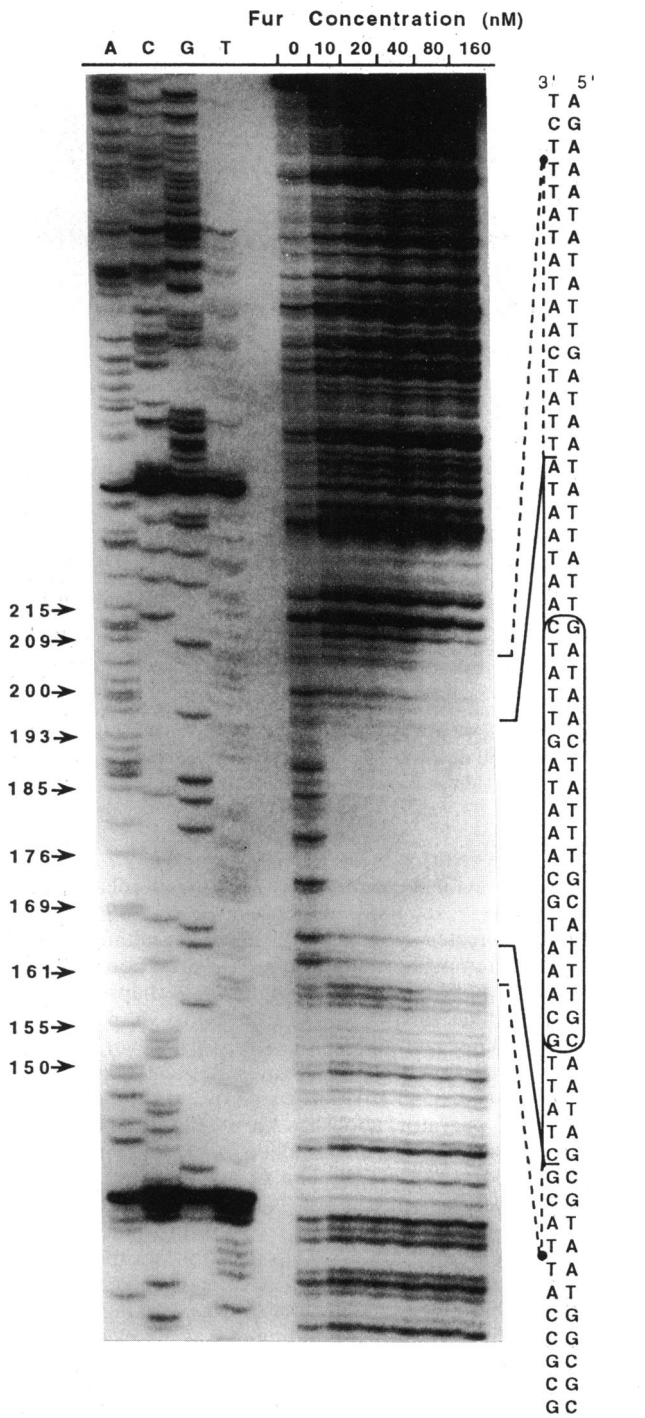

FIG. 6. DNase I protection of the *fepA-fes* intergenic region. The 385-bp *Hin*dIII-*Xho*I fragment containing the *fepA-fes* regulatory region was labeled at its *Hin*dIII end and partially digested with DNase I in the presence of varying concentrations of Fur protein. The nanomolar Fur concentrations used are indicated at the top. The lanes at the left contain a sequence ladder generated by using primer P9 and pITS343-0 as a template. Fragment sizes, in base pairs, corresponding to selected bands in lane A are indicated at the far left. The sequence around the protected area is shown at the right and is oriented so that top to bottom corresponds with right to left in Fig. 3. Solid lines delineate the region of primary protection, and broken lines indicate the region protected only in the presence of higher concentrations of Fur. The proposed iron box is encircled.

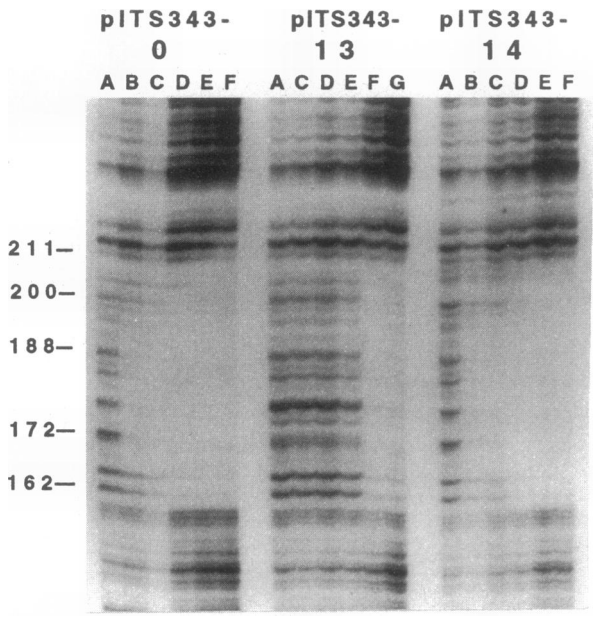

FIG. 7. A comparison of Fur footprints on the operators of pITS343-0 and two mutant derivatives, pITS343-13 and pITS343-14. DNase I footprint analysis was performed as described in the legend to Fig. 6. Fur (monomer) concentrations used were as follows: Lanes A, no Fur; lanes B, 10 nM; lanes C, 20 nM; lanes D, 40 nM; lanes E, 80 nM; lanes F, 160 nM; and lane G, 200 nM. Fragment size markers, in base pairs, are shown at the left.

protection is evident until Fur is present at relatively high concentrations (~160 nM). At this point, both the primary and secondary protected regions are occupied simultaneously.

Previous attempts to isolate single-base mutations within the operator had not been successful (8, 21), perhaps because of the way in which this protein is thought to wrap around its operator, making multiple contacts (19). However, the single A-for-G substitution which inactivates the −35 element of the *fes* promoter (pITS343-16), and which lies at the periphery of the proposed operator, abolishes the regulatory effect of Fur on *fepA* transcription almost as efficiently as the 5-base mutation of pITS343-13 (Fig. 3B). This G is considered part of the iron box consensus, but it is not universally conserved (8, 20), and in at least one well-characterized Fur recognition site (8) it has been replaced with an A. In addition, footprints in the pITS343-16 operator region were indistinguishable from those of the wild-type operator (data not shown), making the severe phenotypic effect somewhat puzzling. It was not clear from the footprints whether this single-base change was causing a slight reduction in the affinity of Fur for its target, that translated to a major functional disturbance, or whether the effect was more indirect, resulting, perhaps, from a regulatory imbalance generated by the lack of polymerase activity at the opposing promoter.

The relative binding affinities of Fur for mutant and normal operators were assessed in vitro by using gel-retardation assays (25, 26). The *Hin*dIII-*Xho*I fragment containing the wild-type operator region and two of its mutant derivatives, from pITS343-13 and pITS343-16, were used in protein binding experiments with concentrations of purified Fur ranging from 1 nM to 500 nM. In our hands, as in previous studies of the aerobactin operon (19, 41, 53), the introduction of Fur to the binding medium containing the wild-type operator fragment initially yields two transitional, lower-mobility species that give way to a maximally shifted fragment at higher concentrations of Fur (Fig. 8). The pITS343-16 operator shows a similar pattern, while pITS343-13 produces only one transitional fragment and a delayed appearance of the fragment with lowest mobility. The precise configuration that leads to each shifted fragment is not known. However, the appearance of all shifted bands depends upon the presence of Fur in a binding medium containing $MnCl_2$, so for the purposes of comparing the relative affinities of the repressor for each of the three operator variants, all shifted fragments were considered to be bound by Fur.

Binding curves were generated for each of the three operator variants by quantitating the amount of DNA in bound and unbound forms at a given Fur concentration and by plotting the proportion of DNA fragment bound versus log Fur concentration (Fig. 8B). The curves generated by the pITS343-0 and pITS343-16 operators were nearly superimposable. Both showed half-maximal binding at Fur (monomer) concentrations between 25 and 30 nM. At 25 nM Fur, the proportion of wild-type (pITS343-0) operator and pITS343-16 operator fragments bound were 42.4(±11)% and 42.0(±15)%, respectively. At 30 nM Fur, the proportions of bound fragment rose to 55(±13)% and 51(±9)% respectively. Although maximal binding of the pITS343-13 operator was not reached in this set of experiments (Fig. 8B), it is evident that half-maximal binding at this operator is approximately one order of magnitude higher: at 250 nM Fur, less than half (47 ± 12%) of the DNA fragment had been bound by the repressor.

The fact that no significant difference could be detected between in vitro binding of the normal operator and that of pITS343-16 suggests that the marked phenotypic effect of this mutation is caused by disruption of the overall architecture of this regulatory region in vivo and is only an indirect result of the base substitution that falls within the operator.

DISCUSSION

The placement of overlapping, divergently oriented promoter regions is now recognized as an organizational scheme that is utilized in a broad range of organisms (5). This can be an expedient arrangement when the genes involved serve related functions and must be coordinately regulated, and it is a unifying factor in the enterobactin synthesis and transport system, the expression of which is largely controlled by three such sets of overlapping promoter-operator regions. Within this gene cluster, however, the details of regulation vary. In the *fepB-entC* control region, the promoters lie back-to-back but do not overlap, and they are controlled by separate Fur-binding sites (8). The *fepD-P43* (12) and *fepA-fes* promoter-operator regions overlap extensively and, particularly in these two cases, there is a strong argument for coordinate transcriptional regulation of the affected operons.

The compact arrangement of the *fepA-fes* intergenic region suggested that it may contain sequences serving dual regulatory roles. To address this possibility, we have combined divergent *fepA'-'phoA* and *fes-entF'-'lacZ* fusions into a bidirectional expression vector and assessed the effects of mutations within the regulatory region. This construct has proven to be an effective tool for monitoring iron-regulated expression of both transcripts simultaneously.

In the course of this project and in a previous study (45), the region between the *fepA* and *fes* coding regions has been sequenced numerous times. It should be noted that our results differ somewhat from those of Lundrigan and Kadner (37). Specifically (reading in the *fepA* direction), multiple T residues

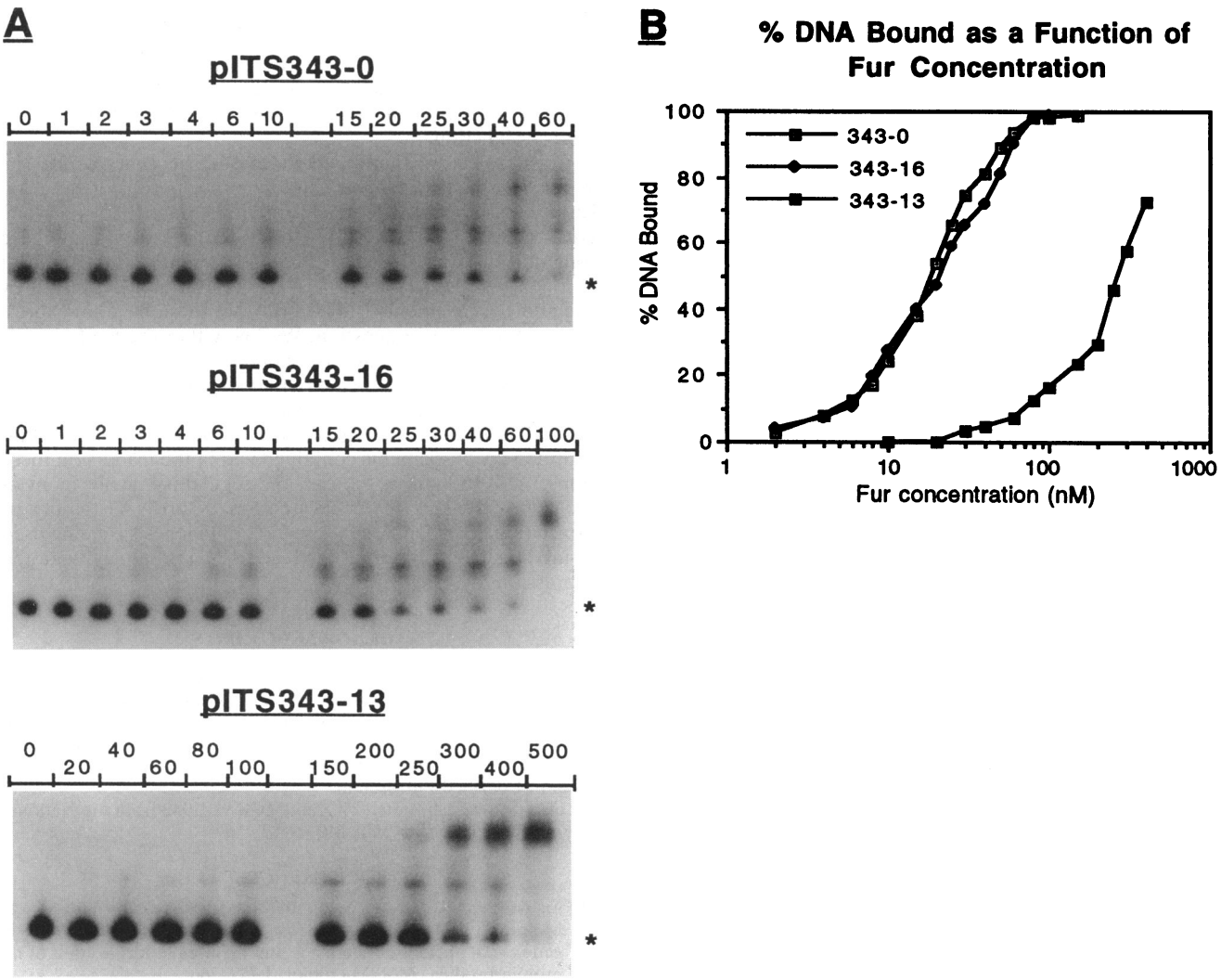

FIG. 8. Gel-shift analysis of the binding affinity of Fur for three different operators. (A) Gel-retardation assays were performed on DNA fragments containing the pITS343-0, pITS343-16, or pITS343-13 operator region. In each case, 0.1 pmol of the *Hin*dIII-*Xho*I operator fragment was used with varying amounts of purified Fur protein. A representative autoradiogram is shown for each of the three operator variants being examined, with nanomolar Fur concentrations indicated at the top of each panel. Asterisks on the right side mark the migration of the unbound DNA fragment. All fragments with lower mobility were considered bound for purposes of quantitation. (B) The relative amounts of DNA present in bound and unbound forms were quantitated by using a PhosphorImager to generate the curves shown here. They represent the averages of three sets of datum points for pITS343-0 and pITS343-16 and of four sets for pITS343-13.

between the start codons of *fepA* and *fes* were omitted from the originally published sequence so that several potential σ^{70} promoter-like sequences were overlooked. Our version of this regulatory sequence has been published (45) and is cataloged under GenBank accession number J04216. The results presented here are based on that sequence.

Deletion and mutational mapping of the *fes-entF* promoter showed that transcription arises from a single promoter, and that sequences upstream of the −35 region contribute very little if anything to expression in the *fes* direction. The *fepA-entD* message, on the other hand, arises from two tandemly arranged iron-regulated promoters. The promoter responsible for most of the *fepA* expression, both in terms of transcript abundance (Fig. 4) and FepA'-'PhoA fusion protein expression (Fig. 3B), is the downstream promoter, designated P1. Whether certain environmental conditions other than iron depletion cause the upstream (P2) promoter to play a more important role in *fepA* expression is not yet known.

A point mutation in the −35 sequence of *fepA* P2 virtually eliminates the less abundant, longer transcript but does not greatly reduce expression of the *fepA'-'phoA* fusion. However, deletions that extend well into the P2 promoter, but which do not yet impinge upon P1 (ΔP32, ΔP54, and ΔP61), show markedly reduced levels of phosphatase expression (Fig. 2B). The pITS343-14 mutation, which substitutes 5 nucleotides upstream of the P1 −35 element, also consistently reduces expression from both the *fepA* and *fes* promoters under low- and high-iron conditions (Fig. 3). These two observations, taken together, suggest a regulatory role for the region that lies immediately upstream of *fepA* P1. The pITS343-14 effect on *fes* expression might be attributed to the fact that the immediate vicinity of the transcription start (+1) has been made more

GC-rich, thus hindering transcription initiation, but the same cannot be said for its effect on the expression of *fepA*, since this mutation is located well upstream of the transcription start and the core promoter determinants for P1.

The region between −37 and −61 (with respect to the major *fepA* transcript) is very AT-rich, and its placement is consistent with the common positioning of *cis*-acting positive regulatory elements, whether activation involves the binding of a transcription factor (16) or the direct interaction of AT-rich upstream DNA with RNAP (48). No regulatory factors besides Fur have been found in the enterobactin synthesis and transport system of *E. coli*, and the possibility of another regulatory element in this case is speculative. However, in regulons other than the enterobactin system (17, 20), Fur is known to act in conjunction with other repressors and transcriptional activators to fine-tune the expression of genes in response to various environmental stimuli.

In the *fepA-fes* intergenic region, a single recognition site for Fur is symmetrically situated over the −35 regions of the two major opposing promoters (Fig. 3). All of the transcripts arising in this region respond strongly to Fur binding at this operator (34, 45). Although there has been no systematic study of the relative strengths of Fur binding sites, this one compares favorably to other characterized sites (8, 18, 20, 28, 52) on the basis of footprinting and gel-retardation assays. However, this operator does not conform in all respects to the consensus iron box. There are well-spaced A-T doublets throughout, and the sequence matches the consensus in 13 of 19 bases, but the region shows none of the dyad symmetry thought to be important in Fur binding.

Another unusual characteristic of this operator is that its activity can be nullified by a single base change. Until now, no single-base substitution mutations within the operator have been detected. However, the mutation in the *fes* −35 region (pITS343-16) abolishes in vivo Fur regulation of the opposing *fepA* transcript (Fig. 3) without affecting the in vitro ability of Fur to bind to the operator (Fig. 8), suggesting that Fur function, in this case at least, may depend upon more than operator recognition and DNA binding per se. A balanced competition between RNAP molecules at this juncture or an interaction between polymerase and Fur (or some other regulatory molecule) may also play a role. The disruption of this equilibrium by eliminating RNAP binding at the *fes* promoter may change the local conformation of the DNA helix in such a way that Fur's ability to bind in vivo is diminished. Alternatively, in the absence of an opposing polymerase, the interaction of RNAP with one of the *fepA* promoters might be enhanced so that Fur can no longer compete effectively. This seems somewhat less likely, since Fur is quite effective in situations when opposing promoters are not a consideration. Moreover, the *fepA* P1 −35 mutation (pITS343-9) consistently amplifies repression of the opposing *fes* transcript under high-iron conditions.

The fact that mutations which inactivate one promoter have such strikingly different effects on the intact opposing promoter under conditions when Fur should be active suggests that there is a fundamental difference in the way that the *fepA* and *fes* promoters respond to Fur repression. Whether these data suggest differences in the regulatory geometry of the two promoters or implicate additional regulatory factors in either or both directions is not yet clear.

The DNA binding studies presented here were all performed in vitro, and it now appears that factors other than the simple interaction of Fur with an isolated target sequence are involved in the activity of this repressor. This compact region is heavily populated with protein recognition sites, and because of this, in vivo footprinting experiments might be difficult to interpret. However, comparative in vivo protection experiments performed under the appropriate conditions should shed light on the interplay between Fur, RNAP, and any additional factors that might be involved in regulation at the *fepA-fes* junction.

This project was undertaken to further characterize the regulation of the *fepA-entD* and *fes-entF* operons at the transcriptional level. Like the divergently transcribed *fepB* and *entCEBA(P15)* transcripts (8), both of these transcripts have long untranslated leaders that show a potential for significant secondary structure, and one consideration not addressed by the above experiments is the effect that these have on expression of the genes in question. We know that the *fepA* portion of the *fepA-entD* message is stabilized in some manner. Although replicative extragenic palindromic sequences positioned 3′ to the *fepA* gene probably play a role in this (1, 45), an additional level of regulation may be provided posttranscriptionally by elements contained within the leaders on these transcripts. In light of the possible regulatory involvement of the leader regions in functions such as mRNA stability or translational efficiency, site-directed mutagenesis is being used to investigate the role that the leaders might be playing in the expression of these genes.

ACKNOWLEDGMENTS

On the basis of their cooperative contributions to the design, execution, analysis, and reporting of the experimental data herein, the first two authors should be given equal credit for this study.

We are grateful to C. Manoil for supplying us with strain CC118 and λTn*phoA*, M. Casadaban for plasmid pMC1403, and J. B. Neilands for his gift of purified Fur protein.

This work was supported by grant MCB 9201942 from the National Science Foundation (to M.A.M.).

REFERENCES

1. **Armstrong, S. K., G. S. Pettis, L. J. Forrester, and M. A. McIntosh.** 1989. The *Escherichia coli* enterobactin biosynthesis gene *entD*: nucleotide sequence and membrane localization of its protein product. Mol. Microbiol. **3**:757–766.
2. **Bachman, B.** 1990. Linkage map of *Escherichia coli* K-12, edition 8. Microbiol. Rev. **54**:130–197.
3. **Bagg, A., and J. Neilands.** 1985. Mapping of a mutation affecting regulation of iron uptake systems in *Escherichia coli* K-12. J. Bacteriol. **161**:450–453.
4. **Bagg, A., and J. Neilands.** 1987. Molecular mechanism of regulation of siderophore-mediated iron assimilation. Microbiol. Rev. **51**:509–518.
5. **Beck, C. F., and R. A. J. Warren.** 1988. Divergent promoters, a common form of gene organization. Microbiol. Rev. **52**:318–326.
6. **Braun, V.** 1985. The unusual features of the iron transport systems of *Escherichia coli*. Trends Biochem. Sci. **10**:75–78.
7. **Brickman, E., and J. Beckwith.** 1975. Analysis of the regulation of *Escherichia coli* alkaline phosphatase synthesis using deletions and φ80 transducing phages. J. Mol. Biol. **96**:307–316.
8. **Brickman, T. J., B. A. Ozenberger, and M. A. McIntosh.** 1990. Regulation of divergent transcription from the iron-responsive *fepB-entC* promoter-operator regions in *Escherichia coli*. J. Mol. Biol. **212**:669–682.
9. **Calderwood, S., and J. Mekalanos.** 1987. Iron regulation of Shiga-like toxin expression in *Escherichia coli* is mediated by the *fur* locus. J. Bacteriol. **169**:4759–4764.
10. **Calderwood, S., and J. Mekalanos.** 1988. Confirmation of the Fur operator site by insertion of a synthetic oligonucleotide into an operon fusion plasmid. J. Bacteriol. **170**:1015–1017.
11. **Casadaban, M. J., J. Chou, and S. N. Cohen.** 1980. *In vitro* gene fusions that join an enzymatically active β-galactosidase segment to amino-terminal fragments of exogenous proteins: *Escherichia coli* plasmid vectors for the detection and cloning of translational

initiation signals. J. Bacteriol. **143**:971–980.
12. **Christoffersen, C. A., T. J. Brickman, and M. A. McIntosh.** Unpublished data.
13. **Cleavenger, C. S., B. A. Ozenberger, and M. A. McIntosh.** Submitted for publication.
14. **Clemens, K. E., and D. J. Pintel.** 1988. The two transcription units of the autonomous parvovirus minute virus of mice are transcribed in a temporal order. J. Virol. **62**:1448–1451.
15. **Cohen, S. N., A. C. Y. Chang, and L. Hsu.** 1972. Nonchromosomal antibiotic resistance in bacteria: genetic transformation of *Escherichia coli* by R-factor DNA. Proc. Natl. Acad. Sci. USA **69**:2110–2114.
16. **Collado-Vides, J., B. Magasanik, and J. D. Gralla.** 1991. Control site location and transcriptional regulation in *Escherichia coli*. Microbiol. Rev. **55**:371–394.
17. **Compan, I., and D. Touati.** 1993. Interaction of six global transcription regulators in expression of manganese superoxide dismutase in *Escherichia coli* K-12. J. Bacteriol. **175**:1687–1696.
18. **de Lorenzo, V., F. Giovannini, S. Wee, and J. B. Neilands.** 1987. Operator sequences of the aerobactin operon of plasmid ColV-K30 binding the ferric uptake regulation (*fur*) repressor. J. Bacteriol. **169**:2624–2630.
19. **de Lorenzo, V., F. Giovannini, M. Herrero, and J. B. Neilands.** 1988. Metal ion regulation of gene expression: *fur* repressor-operator interaction at the promoter region of the aerobactin system of pColV-K30. J. Mol. Biol. **203**:875–884.
20. **de Lorenzo, V., M. Herrero, F. Giovannini, and J. B. Neilands.** 1988. Fur (ferric uptake regulation) protein and CAP (catabolite-activator protein) modulate transcription of *fur* gene in *Escherichia coli*. Eur. J. Biochem. **173**:537–546.
21. **de Lorenzo, V., M. Herrero, and J. B. Neilands.** 1988. pCON4 and pCON5: improved plasmid vectors to study bacterial promoters. FEMS Microbiol. Lett. **50**:17–23.
22. **Fleming, T. P., M. S. Nahlik, and M. A. McIntosh.** 1983. Regulation of enterobactin iron transport in *Escherichia coli*: characterization of *ent*::Mu *d*(Ap^r *lac*) operon fusions. J. Bacteriol. **156**: 1171–1177.
23. **Fleming, T. P., M. S. Nahlik, J. B. Neilands, and M. A. McIntosh.** 1985. Physical and genetic characterization of cloned enterobactin genomic sequences from *Escherichia coli* K-12. Gene **34**:47–54.
24. **Fouser, L. A., and J. D. Friesen.** 1986. Mutations in a yeast intron demonstrate the importance of specific conserved nucleotides for the stages of nuclear mRNA splicing. Cell **45**:81–93.
25. **Fried, M., and D. M. Crothers.** 1981. Equilibria and kinetics of *lac* repressor-operator interactions by polyacrylamide gel electrophoresis. Nucleic Acids Res. **9**:6505–6525.
26. **Garner, M. M., and A. Revzin.** 1981. A gel electrophoresis method for quantifying the binding of proteins to specific DNA regions: applications to components of the *Escherichia coli* lactose operon regulatory system. Nucleic Acids Res. **9**:3047–3060.
27. **Goldberg, M. B., S. A. Boyko, and S. B. Calderwood.** 1990. Transcriptional regulation by iron of a *Vibrio cholerae* virulence gene and homology of the gene to the *Escherichia coli* Fur system. J. Bacteriol. **172**:6863–6870.
28. **Griggs, D. W., and J. Konisky.** 1989. Mechanism for iron-regulated transcription of the *Escherichia coli cir* gene: metal-dependent binding of Fur protein to the promoters. J. Bacteriol. **171**:1048–1054.
29. **Hanahan, D.** 1985. Techniques for transformation of *E. coli*, p. 109–135. *In* D. M. Glover (ed.), DNA cloning, vol. I. IRL Press, Washington, D.C.
30. **Hantke, K.** 1981. Regulation of ferric iron transport in *Escherichia coli* K-12: isolation of a constitutive mutant. Mol. Gen. Genet. **182**:288–292.
31. **Hantke, K.** 1984. Cloning of the repressor protein gene of iron-regulated systems in *Escherichia coli* K-12. Mol. Gen. Genet. **197**:337–341.
32. **Hassan, H. M., and H.-C.H. Sun.** 1992. Regulatory roles of Fnr, Fur, and Arc in expression of manganese-containing superoxide dismutase in *Escherichia coli*. Proc. Natl. Acad. Sci. USA **89**:3217–3221.
33. **Hawley, D. K., and W. R. McClure.** 1983. Compilation and analysis of *Escherichia coli* promoter DNA sequences. Nucleic Acids Res. **11**:2237–2255.
34. **Hunt, M. D., and G. S. Pettis.** Unpublished data.
35. **Kunkel, T.** 1985. Rapid and efficient site-specific mutagenesis without phenotypic selection. Proc. Natl. Acad. Sci. USA **82**:488–492.
36. **Lankford, C. E.** 1973. Bacterial assimilation of iron. Crit. Rev. Microbiol. **2**:273–331.
37. **Lundrigan, M. D., and R. J. Kadner.** 1986. Nucleotide sequence of the gene for the ferrienterochelin receptor FepA in *Escherichia coli*. J. Biol. Chem. **261**:10797–10801.
38. **Manoil, C., and J. Beckwith.** 1985. Tn*phoA*: a transposon probe for protein export signals. Proc. Natl. Acad. Sci. USA **82**:8129–8133.
39. **Miller, J. H.** 1972. Experiments in molecular genetics, p. 352–355. Cold Spring Harbor Laboratory, Cold Spring Harbor, N.Y.
40. **Nahlik, M. S., T. J. Brickman, B. A. Ozenberger, and M. A. McIntosh.** 1989. Nucleotide sequence and transcriptional organization of the *Escherichia coli* enterobactin biosynthesis cistrons *entB* and *entA*. J. Bacteriol. **171**:784–790.
41. **Neilands, J. B.** 1981. Iron absorption and transport in microorganisms. Annu. Rev. Nutr. **1**:27–46.
42. **Niederhoffer, E. C., C. M. Naranjo, K. L. Bradley, and J. A. Fee.** 1990. Control of *Escherichia coli* superoxide dismutase (*sodA* and *sodB*) genes by the ferric uptake regulation (*fur*) locus. J. Bacteriol. **172**:1930–1938.
43. **Norrander, J., T. Kempe, and J. Messing.** 1983. Construction of improved M13 vectors using oligodeoxynucleotide-directed mutagenesis. Gene **26**:101–106.
44. **Ozenberger, B. A., T. J. Brickman, and M. A. McIntosh.** 1989. Nucleotide sequence of *Escherichia coli* isochorismate synthetase gene *entC* and evolutionary relationship of isochorismate synthetase and other chorismate-utilizing enzymes. J. Bacteriol. **171**: 775–783.
45. **Pettis, G. S., T. A. Brickman, and M. A. McIntosh.** 1988. Transcriptional mapping and nucleotide sequence of the *Escherichia coli fepA-fes* enterobactin region: identification of a unique iron-regulated bidirectional promoter. J. Biol. Chem. **263**:18857–18863.
46. **Pettis, G. S., and M. A. McIntosh.** 1987. Molecular characterization of the *Escherichia coli* enterobactin cistron *entF* and coupled expression of *entF* and the *fes* gene. J. Bacteriol. **169**:4154–4162.
47. **Prince, R. W., D. G. Storey, A. I. Vasil, and M. L. Vasil.** 1991. Regulation of *toxA* and *regA* by the *Escherichia coli fur* gene and identification of a Fur homologue in *Pseudomonas aeruginosa* PA103 and PA01. Mol. Microbiol. **5**:2823–2831.
48. **Ross, W., K. K. Gosink, J. Salomon, K. Igarashi, C. Zou, A. Ishihama, K. Severinov, and R. L. Gourse.** 1993. A third recognition element in bacterial promoters: DNA binding by the α subunit of RNA polymerase. Science **262**:1407–1413.
49. **Sambrook, J., E. F. Fritsch, and T. Maniatis.** 1989. Molecular cloning: a laboratory manual, 2nd ed., p. 15.20–15.26. Cold Spring Harbor Laboratory, Cold Spring Harbor, N.Y.
50. **Shea, C. M., and M. A. McIntosh.** 1991. Nucleotide sequence and genetic organization of the ferric enterobactin transport system: homology to other periplasmic binding protein-dependent systems in *Escherichia coli*. Mol. Microbiol. **5**:1415–1428.
51. **Tardat, B., and D. Touati.** 1991. Two global regulators repress the anaerobic expression of MnSOD in *Escherichia coli*: Fur (ferric uptake regulation) and Arc (aerobic respiration control). Mol. Microbiol. **5**:455–465.
52. **Tardat, B., and D. Touati.** 1993. Iron and oxygen regulation of *Escherichia coli* MnSOD expression: competition between the global regulators Fur and ArcA for binding to DNA. Mol. Microbiol. **9**:53–63.
53. **Wee, S., J. B. Neilands, M. L. Bittner, B. C. Hemming, B. L. Haymore, and R. Seetharam.** 1988. Expression, isolation and properties of Fur (ferric uptake regulation) protein of *Escherichia coli* K 12. Biol. Metals **1**:62–68.